Singular Vectors, Predictability and Ensemble Forecasting for Weather and Climate

T. N. Palmer and Laure Zanna

Atmospheric, Oceanic and Planetary Physics, Dept of Physics, University of Oxford, Clarendon Laboratory, Parks Road, Oxford OX1 3PU, UK

E-mail: `t.n.palmer@atm.ox.ac.uk, zanna@atm.ox.ac.uk`

Abstract.
The local instabilities of a nonlinear dynamical system can be characterised by the leading singular vectors of its linearized operator. The leading singular vectors are perturbations with the greatest linear growth and are therefore key in assessing the system's predictability. In this paper, the analysis of singular vectors for the predictability of weather and climate and ensemble forecasting is discussed. An overview of the role of singular vectors in informing about the error growth rate in numerical models of the atmosphere is given. This is followed by their use in the initialisation of ensemble weather forecasts. Singular vectors for the ocean and coupled ocean-atmosphere system in order to understand the predictability of climate phenomena such as ENSO and meridional overturning circulation are reviewed and their potential use to initialise seasonal and decadal forecasts is considered. As stochastic parameterisations are being implemented, some speculations are made about the future of singular vectors for the predictability of weather and climate for theoretical applications and at the operational level.

1. Introduction

The leading singular vectors of a nonlinear dynamical system's tangent propagator are strongly related to the system's local finite-time instabilities and therefore play a key role in characterising and assessing the system's predictability. As discussed below, the corresponding singular values can be much larger than the system's Lyapunov exponents if, as is often the case in fluid flow, the tangent propagator is non normal (Trefethen et al. 1993, Farrell & Ioannou 1996). The establishment of singular vectors decomposition and its theory can be traced back to early work by Beltrami (1873) and Jordan (1874). Pioneering work by Farrell and coauthors applied these ideas to atmospheric dynamics by analyzing singular vectors and associated transient growth in, for example, Couette flow (Farrell 1982), mid-latitude cyclogenesis (Farrell 1988, Farrell 1989), forecast error growth in atmospheric models (Farrell 1990), stability of stratified flows (Farrell & Ioannou 1993a, Farrell & Ioannou 1993b) and the dynamics of mid-latitude atmospheric jets (Farrell & Ioannou 1995). The initial conditions leading to the largest amplification at a given time are often referred to as optimal initial conditions and correspond to the leading singular vectors (Farrell & Ioannou 1996). The links between singular vectors and a system's predictability (including error growth and sensitivity) are discussed in more detail below (see Section 2).

Over the last 20 years or so, there has been a revolution in the way in which weather forecasts are made: whereas earlier such forecasts were essentially deterministic, nowadays a prediction system is run in ensemble mode to produce probabilistic predictions. Each ensemble member samples an initial state consistent with estimates of uncertainty in the initial state.

From the earliest days of ensemble weather prediction, it was realised that naive estimates of initial uncertainty e.g. formed by randomly perturbing the weather observations and running the data assimilation system with such perturbed observations, led to underdispersive ensembles. This was a serious problem because whilst in the past a user was aware that deterministic forecasts should be taken with "a pinch of salt", there was an expectation that a probabilistic forecast, where forecast probabilities were close to 100% should be believed. It was realised that the reason for such underdispersion lay in multiple unrepresented sources of forecast uncertainty. For these reasons, discussed in more detail below (see Section 3), singular vectors became a useful tool for initialising ensemble weather forecasts (e.g., Errico 1991, Hartmann et al. 1995, Buizza & Palmer 1995).

Since then, singular vector has been extended from the atmosphere only, to the ocean and to the coupled ocean-atmosphere system. In turn, singular vectors have also been used to understand the predictability of the coupled system, and to initialise ensemble forecasts on the seasonal and decadal timescales (Section 3).

On the other hand, as the assimilation schemes which ingest raw observations to determine initial states in numerical weather prediction become more sophisticated, the

nature of the unrepresented sources of forecast uncertainty are beginning to be better understood. Most important of these is model uncertainty. As new stochastic methods to represent model uncertainty start to be developed, the role of singular vectors to initialise ensemble forecasts needs to be re-evaluated against more straightforward Monte Carlo methods. The role of singular vectors as a key tool to understand the dynamical instabilities and theoretical predictability of the climate system will remain. However, as a tool in practical ensemble forecasting, will singular vectors become redundant one day?

2. Singular Vectors and the Predictability of Nonlinear Dynamical Systems

Start by considering a trajectory T in state space defined by the nonlinear evolution equation

$$\dot{X} = F[X] \tag{1}$$

and initial state X_0. A small perturbation δx to X_0 evolves on T according to

$$\delta \dot{x} = J \delta x \tag{2}$$

where the Jacobian operator J is defined as

$$J = dF/dX \tag{3}$$

Since $F[X]$ is at least quadratic in X, then J is at least linearly dependent on X, indicating that the growth of small perturbations varies both along T and with respect to X_0.

If (1) is taken as the basis of weather and climate prediction, then whilst equation 1 is formally deterministic, inevitable uncertainties in X_0 (associated with the raw observations, with the method used to assimilate observations into model variables X, and in the model equations themselves) means that predictions should be considered as probabilistic rather than deterministic.

As such, a more relevant prognostic variable is the probability density function $\rho(X, t)$ defined as follows: given some volume V in state space then $\int_V \rho(X, t)dV$ is the probability that the true initial state X at time t lies in V.

It turns out ($1994a$, $1994b$) that formal solution of the Liouville equation

$$\frac{\partial \rho}{\partial t} + \frac{\partial (\dot{X}\rho)}{\partial X} = 0 \tag{4}$$

which evolves $\rho(X, t_0)$, can be written

$$\rho(X, t) = \rho(X', t_0) / \exp\{\int_{t_0}^{t} \text{tr}[J(t')]dt'\} \tag{5}$$

Using the identity $\det \exp A = \exp \text{tr} A$ then

$$\rho(X, t) = \rho(X', t_0) / \det M(t, t_0) \tag{6}$$

where

$$M(t, t_0) = \exp \int_{t_0}^{t} J(t')dt' \tag{7}$$

is the so-called forward tangent propagator, mapping a perturbation $\delta x(t_0)$ along T to

$$\delta x(t) = M(t, t_0)\delta x(t_0) \tag{8}$$

Interestingly, and perhaps surprisingly at first sight, the Liouville equation can be solved exactly knowing the initial value $\rho(X', t_0)$ and the tangent propagator M. This relates to the fact that the Liouville equation is linear in ρ even though equation 1 is nonlinear. In practice, however, $\rho(X', t_0)$ is not well known, and equation 6 is very difficult to solve directly.

The propagator M determines the local flow-dependent instabilities of the system. First, consider a Euclidean inner product $\langle \ldots, \ldots \rangle$ so that for any perturbation vectors δx, δy

$$\langle \delta x, \delta y \rangle = \delta x \cdot \delta y \tag{9}$$

where $\cdot$ is the standard Euclidean dot product acting on the vectors δx, δy.

In terms of this, the adjoint tangent propagator M^* is defined by

$$\delta y(t') = M^*(t', t)\delta y(t) \tag{10}$$

where

$$\langle \delta y, M\delta x \rangle = \langle M^*\delta y, \delta x \rangle \tag{11}$$

The inner product $\langle \ldots, \ldots \rangle$ defines a norm. The perturbation which satisfies

$$\max_{\delta x(t_0)} \frac{\langle \delta x(t), \delta x(t) \rangle}{\langle \delta x(t_0), \delta x(t_0) \rangle} \tag{12}$$

is the leading eigenvector of

$$M^*M\delta x(t_0) = \lambda^2 \delta x(t_0) \tag{13}$$

The eigenvectors of M^*M are known as the left or initial singular vectors of M, and the corresponding eigenvectors of MM^* are known as the right or evolved singular vectors of M. As is easily shown, the initial singular vectors are mapped to the evolved singular vectors by the tangent propagator M. The associated eigenvalues of M^*M are known as singular values of M. In general, M is not a normal operator i.e. $M^*M \neq MM^*$ implying that the eigenvectors of M do not form an orthogonal set (trivially, the singular vectors of M do). As a result, the singular values of M can far exceed its eigenvalues - an explicit example is discussed below. The dominant left singular vectors of M (i.e. with largest singular value) provide a locally unstable subspace in the tangent space at t_0. This definition does not agree with definitions based Lyapunov vectors however it a consistent definition and one proven useful for predictability studies.

Because of this singular vector growth can be substantially greater than that associated with the asymptotic growth rate of small perturbations giving by the system's

leading Lyapunov exponent. A dynamical system's Lyapunov exponents can be defined as

$$\bar{\lambda}_i = \lim_{t \to \infty} \lim_{d_i(0) \to 0} \frac{1}{t} \ln \frac{d_i(t)}{d_i(0)} \tag{14}$$

where d_i is the eigenvalue of the ith eigenvector of the operator

$$\lim_{t \to \infty} \frac{1}{t} [MM^T]^{1/2t} \tag{15}$$

These eigenvectors correspond to realisations of evolved singular vectors, for asymptotically long optimisation times, ie for trajectories that, for all practical purposes, cover the entire attractor.

Fig 1 illustrates schematically the crucial difference between Lyapunov and singular vector growth in a two-dimensional non-self adjoint system in a stationary system (Palmer 2000). Here ξ_1 and ξ_2 are non-orthogonal eigenvectors of J. It will be assumed that the real part of these eigenvalues is negative. Hence the amplitude of a perturbation $\mu(t)$ which projects onto either ξ_1 or ξ_2 will decay with time. η_1 and η_2 denote adjoint eigenvectors: η_1 is normal to ξ_2 and η_2 is normal to ξ_1. A perturbation $\nu(t)$ which projects onto η_1 will grow over a finite time interval, even though both eigenvalues are negative. On the other hand, after this initial transient the perturbation $\nu(t)$ will increasingly project onto the leading eigenvector ξ_1 and will asymptotically decay at a rate given by the real part of the negative eigenvalue of ξ_1. The amount ν can grow over a finite time interval is linked to the angle between ξ_1 and ξ_2, i.e. the degree of non-self adjointness of the dynamical operator. The value of this parameter is independent of the value of the eigenvalues.

It can be shown Ehrendorfer (1994a, 1994b) that the determinant of M, a key element in the solution of the Liouville equation (see equation 6) is determined by the product of all the corresponding singular values. Hence, the singular vectors of a nonlinear system are intimately related to the system's predictability.

This relation can be made more explicit through the choice of inner product. In the theory of data assimilation (e.g. 4DVAR; Talagrand. & Courtier 1987, Thépaut & Courtier 1991), statistical uncertainty in the initial state is represented by a Gaussian PDF with covariance matrix A. The norm of the singular vectors can easily be made consistent with A. Hence, a vector which instead of equation 12, satisfies

$$\max_{\delta x(t_0)} \frac{\langle \delta x(t), \delta x(t) \rangle}{\langle \delta x(t_0), A^{-1} \delta x(t_0) \rangle} \tag{16}$$

i.e. with unit initial amplitude defined with respect to the metric A can be shown to be the leading eigenvector of the generalised eigenvector equation

$$M^* M \delta x(t_0) = \lambda_A A^{-1} \delta x(t_0) \tag{17}$$

which can be solved using a generalised Davidson algorithm (Barkmeijer et al. 1998). In practice, the energy norm provides a reasonable approximation to the more complex analysis error covariance norm for singular vector computations (Lawrence et al. 2009, Palmer et al. 1998). A key property of energy norm singular vectors
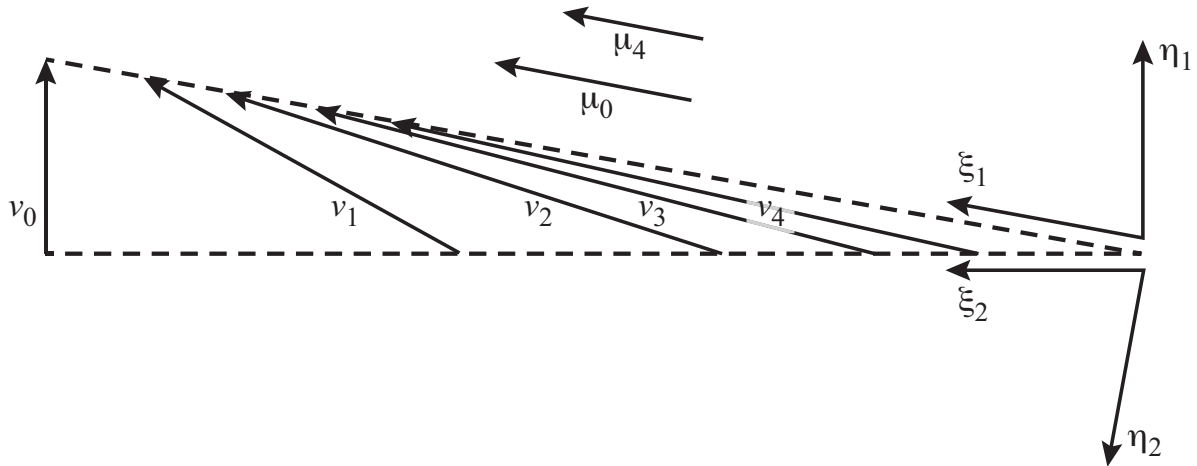
Figure 1. This diagram illustrates schematically the crucial difference between eigenvector and singular vector growth. From Buizza & Palmer (1995)

(mimicking those from more accurate A norm singular vectors, is upscale growth. An example of an energy metric singular vector for the atmosphere is shown in Fig 2 (from Buizza & Palmer (1995)).

The singular vector analysis described above is also relevant in describing the system's response to some imposed forcing (which, in the current context, is presumed to represent model error). If we modify equation 2 so that

$$\dot{\delta x} = J\delta x + f \tag{18}$$

then, using the tangent propagator M, the solution to this equation over the finite time interval $[t_0, t]$ can be written

$$\delta x = M(t, t_0)\delta x(t_0) + \int_{t_0}^{t} M(t, t')f(t')dt' \tag{19}$$

If f is time-independent over $[t_0, t]$, then, setting $\delta x(t_0) = 0$

$$\delta x(t) = \mathcal{M}(t, t_0)f \tag{20}$$

where

$$\mathcal{M}(t, t_0) = \int_{t_0}^{t} M(t, t')dt' \tag{21}$$

Singular vectors of $\mathcal{M}$ represent optimal forcing structures. In principle they could have value in representing model error. In practice the estimation of such singular vectors is computationally demanding.

3. SVs and Ensemble Forecasting for Weather and Climate

3.1. Numerical Weather Prediction

Traditionally, numerical weather prediction has been considered a deterministic initial value problem (Bjerknes 1904). However, the realisation of the chaotic nature of
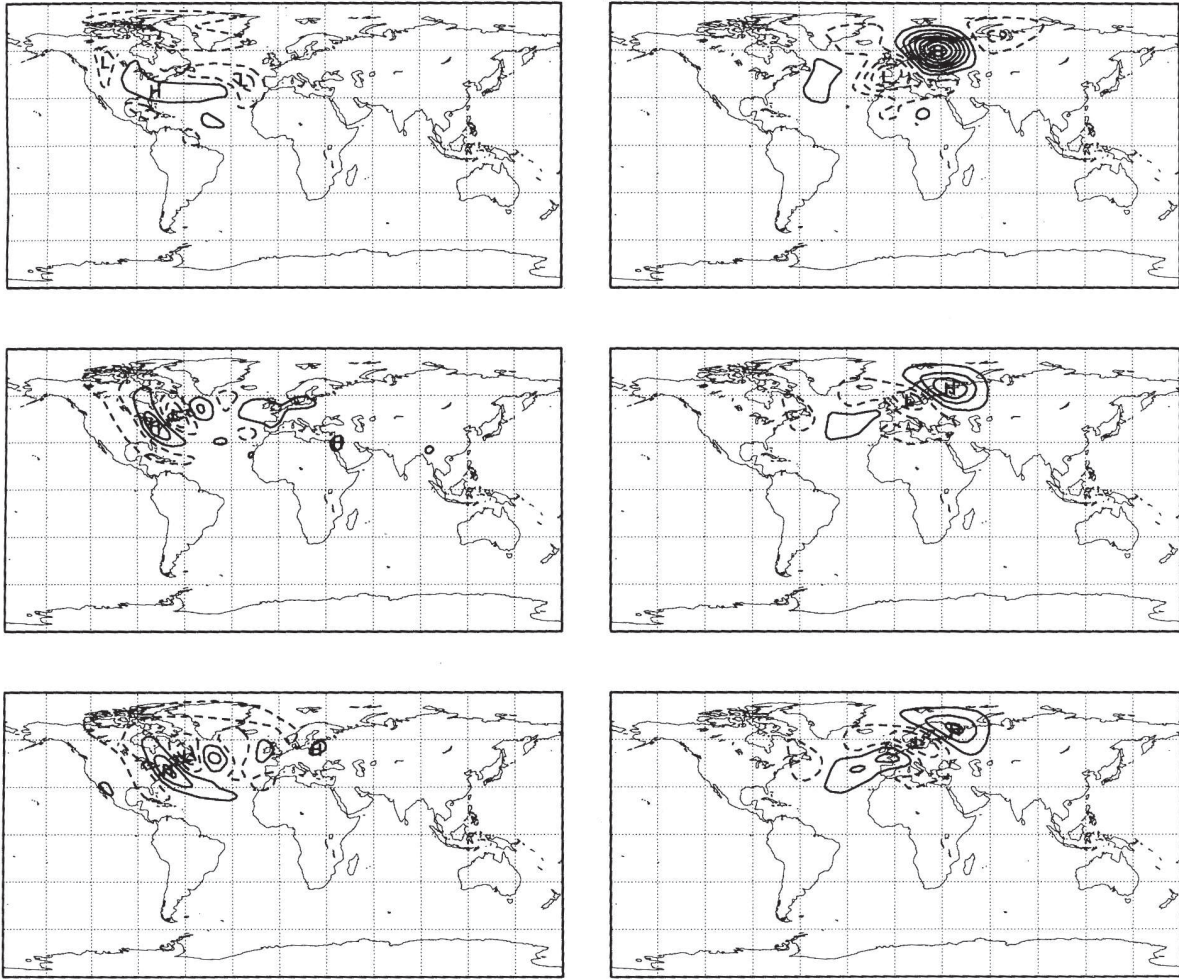
Figure 2. Streamfunction of the dominant singular vector of the atmospheric tangent propagator M, calculated using a primitive equation numerical weather prediction model for a three day trajectory portion made from initial conditions of 9 January 1993 at: (a), (d) 200hPa; (b)(e) 700hPa; (c)(f) 850hPa. The quantities (a)-(c) are at initial time, in (d)-(f) at final time. The contour interval at optimisation time. The contour interval at optimisation time is 20 times larger than at initial time. From Buizza & Palmer (1995)

atmospheric dynamics Lorenz (1963, 1969) made it clear that deterministic forecasts would be unreliable due to the amplification of inevitable uncertainties in forecast initial conditions.

Of course a simple way of making a deterministic forecast reliable would be to 'dress' it *a posteriori* using a probability distribution of forecast error constructed from a large sample of previous forecast errors. However, the utility of such a probabilistic system would be rather limited. Since the underpinning dynamical equations are nonlinear, then the Jacobian of the linearised equations must vary according to position on the attractor. For forecasts in the part of the attractor where the leading singular values are relatively small, this 'climatological' pdf of forecast error provides a pessimistic estimate

of the likely error of a deterministic prediction, whilst for deterministic forecasts in the part of the attractor where the leading singular values are large, the 'climatological' pdf provides an optimistic estimate of deterministic forecast error. This variation in predictability with position on the attractor is well known to meteorologists. During a spell of settled anticyclonic weather, small uncertainties in the initial conditions of a weather forecast are likely to make little difference to the forecast of continued settled weather. By contrast, as a small scale cyclonic disturbance develops over the ocean, a small change to initial conditions can make a substantial difference to the subsequent intensity and path of the resulting storm.

For this reason, it is better to start out with the objective of estimating flow-dependent probability distributions of future weather by dynamical methods. This can be achieved by ensemble prediction methods. With such methods, it is hoped to be able to reliably discriminate between predictable and unpredictable flows. Hence in a situation where a weather event is forecast with probability close to 100%, a forecast user should really be able to rely on the forecast. By contrast in a situation where a weather event is forecast with probability close to the climatological frequency of the event, the forecast user will know that the event has no predictability in this particular situation.

In theory, ensemble prediction should be straightforward. Sample randomly the pdf of initial error. Repeat N times. Integrate the resulting N initial states in time and produce a frequentist estimate of forecast probability for any variable or event of interest (probability of rain, probability that temperature is below freezing, probability of wind exceeding the climatological 99% percentile. This is essentially Monte Carlo weather forecasting. Historically, this method has failed to produce useful results.

To understand this, it should be recalled that the climate system is effectively an infinite dimensional system, describing planetary-scale Rossby waves on the one hand, to small scale turbulent motion e.g. associated with individual clouds, on the other. The energy associated with these various scales, has a power law structure, shallowing from a '-3' slope for large rotationally constrained scales to '-5/3' for scales whose structure is more three dimensional (Nastrom & Gage 1985). Simulating this '-5/3' spectrum is a challenging problem. Not least it implies that simulations, even of the large-scale rotationally dominated aspects of the flow can be sensitive to smaller scale motions, as envisaged in Lorenz (1969)'s paradigm. In practice this means that weather forecasts can be sensitive to the parametrised processes in the model, perhaps most importantly to the parametrisation of deep convection.

A weather forecast model is not only used to integrate the state of the atmosphere from $t = 0$ to some forecast time $t = T > 0$, it also plays a key role in determining the state at $t = 0$, given observations of the atmosphere at $t \leq 0$. For example, in variational data assimilation (e.g. Courtier et al, 1994, 1998) a cost function is minimised which combines current observations with an recent earlier estimate of an initial state, propagated forward in time using the tangent propagator. An ensemble of data assimilations can be created by randomly perturbing the input observations

according to their known error characteristics (an *in situ* thermometer has known accuracy, so too a satellite radiometer). However, this leads to very underdispersive forecast ensembles (Buizza et al. 1999), i.e. to ensembles in which the spread of the ensemble is substantially smaller than the (ensemble-mean) forecast error. The reason for this is that there are many unrepresented sources of uncertainty not explicitly represented in a Monte Carlo forecast. Perhaps the most important of these is the uncertainty in the weather forecast model used to assimilate the observations and produce the forecast itself. Because of the potential for rapid upscale propagation of error from the parametrised to the large scales, errors in the weather forecast model contribute significantly to the initial error.

It was always possible to inflate artificially estimates of observation uncertainty to ensure that the ensemble spread at some target forecast time (e.g. t=5 days) was about right (i.e. was balanced against a typical ensemble-mean forecast error, but this meant that the forecast ensemble was very overdispersive in the early forecast range, and moreover did not discriminate between predictable and unpredictable flows very effectively. Such inflated ensemble systems were therefore not very useful in practice.

The first operational ensemble prediction systems (for the medium and extended range) used such artificially inflated initial perturbations in the mid 1980s (Murphy & Palmer 1986). However, in producing a more discriminating ensemble forecast system for the European Centre for Medium Range Weather Forecasts in the late 1980s, a method based on singular vectors was developed (Buizza & Palmer 1995, Mureau et al. 1993).

A key motivation for the development of this method arose from a study of the large-scale flows associated with large and small medium range forecast error (Palmer 1988). Flows with a positive component of the Pacific North American (PNA) teleconnection pattern were shown to be associated with relatively small medium range forecast error, whilst those with a negative component of this teleconnection pattern were shown to be associated with relatively large medium range forecast errors. In collaboration with Zuojun Zhang and Brian Hoskins at Reading University, it was shown that the reason errors were amplifying was not because the dominant barotropic eigenvectors of the positive PNA flows had smaller eigenvalues (and therefore were more asymptotically stable - in fact the opposite was true) but because the leading eigenvectors associated with the positive PNA flow were more orthogonal (i.e. the dynamical barotropic operator of the linear perturbation system was more self adjoint) than the leading eigenvectors of the negative PNA flow. The study of predictability during spells of positive and negative PNA, illustrated the relevance of the schematic figure 1.

This analysis showed that so-called normal mode instability was an inadequate and inappropriate methodology to analyse the predictability of atmospheric flows. This was completely consistent with the pioneering work of Farrell and his coworkers (e.g., Farrell & Ioannou 1996, Farrell 1985) who concluded that normal mode instability was an inadequate and inappropriate method to analyse the dynamical instability of atmospheric flows.

In the early days of ensemble weather prediction, there were no techniques to

estimate the role of model error, not only during the forecast integration period, but also during the data assimilation cycle. As an alternative strategy, the use of the leading singular vectors of the forward tangent propagator M to generate initial ensemble perturbations was considered and found successful (Mureau et al, 1993). The existence of an adjoint propagator M^*, needed for 4DVAR, made singular vector computations possible from a primitive equation model, using a Lanczos algorithm. In principle it is possible to supplement the singular vectors of M with singular vectors of $\mathcal{M}$, the latter defining optimal model error forcing structures (see equation 21). However, in practice the computation of the latter proved too computationally burdensome in an operational environment.

Providing these singular vectors were estimated with respect to the analysis error covariance metric A then at optimisation time, these singular vectors would correspond to the leading eigenvectors of the forecast error covariance matrix, and in some sense would bound possible error growth. However, estimating A^{-1} is computationally complex and hence surrogate analysis error covariance matrices were sought. Of these the so-called energy metric proved most relevant (Palmer et al. 1998). With respect to the energy metric, the singular vectors evolved from sub-synoptic to synoptic scales. Such an upscale evolution is exactly what one would expect of the evolution of analysis errors - a reasonably observational network would constrain well scales which are much larger than the network scale, and poorly constrain scales either close to or below the network scale. As these small scale errors grow, they propagate upscale and affect the key baroclinic modes of the atmosphere.

The ECMWF EPS became operational in 1992 with initial perturbations which combined initial singular vectors from $t = 0$ and evolved singular vectors from $t - 2$ days (Molteni et al. 1996). In 1999 this method was supplemented by a stochastic parametrisation of sub-grid processes to represent model error (Buizza et al. 1999).

More recently still a method to produce an ensemble of data assimilations (EDA) has been developed at ECMWF (Bonavita 2011). The primary motivation for this development was not in fact for the EPS, but rather to provide flow-dependent background error covariance matrices for 4DVAR. It was found important to include the stochastic representation of model uncertainty in order that the spread of the ensemble of data assimilation correspond well with the mean analysis increment. With the development of stochastic parametrisation as an explicit tool to estimate model uncertainty (Palmer 2001, Palmer 2012), it may be possible to return to the original Monte Carlo type concept and sample randomly from EDA, thus dropping altogether the singular vector approach. However, recent studies (Martin Leutbecher, personal communication 2012) shows this is not entirely possible, and the latest version of ECMWF EPS initial perturbations combines EDA with singular vectors. Whether this hybrid approach provides a long-term strategy for medium-range ensemble perturbations, time will tell.

3.2. **El Niño and Seasonal Forecasting**

Despite the chaotic nature of the atmosphere, seasonal and interannual fluctuations resulting from coupled interactions can be predictable due the memory of the ocean and/or land. A seasonal forecast, similarly to a weather forecast, is an initial value problem and depends on the initial state. Predictability is lost as initial uncertainties grow in time. An example of such coupled ocean-atmosphere interaction is the El Niño-Southern Oscillation (ENSO) phenomenon. ENSO refers to an irregular interannual oscillation of large-scale sea surface temperature (SST) and associated air pressure in the tropical Pacific. While the large-scale fluctuations of ENSO are localised to the tropical Pacific, their influence can affect other regions of the Pacific and other basins via atmospheric teleconnections influencing surface temperature, rainfall and wind (e.g., Gu & Philander 1997, Lau & Nath 2000). Long-term variability of ENSO is believed to be only weakly chaotic (e.g., Suarez & Schopf 1988, Penland & Sardeshmukh 1995, Moore & Kleeman 1999) and exhibits some predictability up to a year ahead.

Unlike weather forecasts, seasonal prediction systems require integrations of the nonlinear equations for the oceanic and atmospheric components, both essential to simulate ENSO variability adequately. The skill of ENSO dynamical prediction is seasonally dependent (Cane 1986) and affected by several sources of errors including initial conditions, ocean model parametrisations or the unpredictable high-frequency forcing of the atmosphere (e.g., Chen et al. 1995, Rosati et al. 1997, Latif et al. 1998, Moore & Kleeman 1997a). ENSO dynamics may be highly non-normal such that singular vectors can provide a good measure for error growth on seasonal timescales (e.g., Moore & Kleeman 1999, Chen et al. 1997, Penland & Sardeshmukh 1995, Thompson & Battisti 2000, Thompson & Battisti 2001). Over the years, studies of tropical Pacific singular vectors using the observed record, simple models and general circulation models (GCMs) have highlighted the importance of the ocean initial state for ENSO predictions. Singular vector analysis has also demonstrated the dependence of the optimal error growth on the seasonal cycle, ENSO phase and lead time for prediction.

Early studies by Blumenthal (1991) and Xue et al. (1994) showed that the SST anomaly pattern leading to the optimal error growth (equivalent to the leading singular vector) is similar to the ENSO pattern of idealised models. They found that the largest growth rate occurs in spring, consistent with suggestions that springtime is favorable for self organisation of perturbations (Philander 1986). Error growth in SST anomalies during the spring appears to be associated with non-normal energy growth such that initial errors in tropical Pacific SSTs would have a significant impact on the accuracy of a seasonal forecast of ENSO if the dynamical prediction begins around springtime. In coupled models of intermediate-complexity, Moore & Kleeman (1996, 1997a, 1997b) examined the dynamics of error growth and predictability finding that the conditions for error growth are favorable in the central Pacific where SSTs are warm, and where changes in SST are sensitive to anomalies of oceanic thermocline. Overall, seasonal forecasts beginning in spring tend to be less skillful than other forecasts.

The analysis of the singular vectors for ENSO prediction is clearly valuable however their computational cost becomes expensive for coupled GCMs (CGCMs) as those used in seasonal forecasting. Besides their computational cost, the value of singular vectors in CGCMs is limited as the fastest growing modes are due to weather instabilities which are irrelevant for the coupled instabilities of the ENSO system. The weather instabilities will grow at a faster rate than any other instability in the coupled model and will dominate the singular vector spectrum. Kleeman et al. (2003) proposed a methodology to average out the atmospheric noise by running a large ensemble of integrations with a coupled GCM for specific initial states and calculate only the relevant part of the singular vector spectrum for the coupled response. The main motivation of the technique lies in the fact that the ensemble-mean propagator of a linear stochastic differential equation with additive stochastic forcing (in this case the atmospheric noise) is equal to the propagator of the system without stochastic forcing (the coupled ENSO variability). If the atmospheric stochastic forcing can be removed, the " ensemble-mean" response would provide the appropriate response for the non-stochastically forced system. In Tang et al. (2006), this technique was applied to a fully coupled GCM to investigate the error growth associated with ENSO forecasts. Similarly to other studies, Tang et al. (2006) found that the error growth of prediction is strongly influenced by the phase of the ENSO cycle. In general, the large growth rates of the fastest-growing singular vectors occur during the onset and the peak of El Niño. On the other hand, relatively small growth rates occurs during the onset and the peak of La Niña. Their results suggest that El Niño maybe be less predictable than La Niña. However, unlike other studies, the authors show that initial information in SST plays a more significant role than subsurface temperatures information for predicting the tropical Pacific SST. This result contradicts work pointing out the importance of subsurface information for ENSO prediction (e.g., Latif & Graham 1992, Neelin et al. 1998). There are several possible explanations for the discrepancies. One of them is that the behavior of the interannual ENSO cycles is model dependent. Some models exhibit strong subsurface feedbacks associated with the delay-oscillator mechanism while others show strong surface layer feedback associated with SST zonal advection. Yet, theory and most models seem to suggest an important role of the oceanic initial state in ENSO forecasts.

The derived singular vector patterns from Tang et al. (2006) could help the initialisation of ensemble seasonal forecast as it avoids weather instabilities and does not require an adjoint or a tangent linear model. However the methodology remains computationally expensive to implement in operational forecast systems as it requires to run large ensembles of coupled climate models. Additional empirical methods have been developed for CGCMs (see Tziperman et al. (2008) discussed below) and applied to ensemble seasonal forecasting using coupled hybrid models (e.g., Kug et al. 2010) but none of these techniques has yet been implemented in coupled GCMs or tested against current operational seasonal forecast.

Currently, the operational seasonal forecast system at ECMWF (System 4) consist of ensembles of integrations of coupled ocean-atmosphere GCMs. It uses

perturbed atmospheric stochastic physics to account for model uncertainties, and uses for initial conditions a combination atmospheric singular vectors and an ensemble of ocean reanalysis (NEMOVAR). A 5-member ensemble of NEMOVAR is created using perturbed wind forcing and the ocean reanalyses are further perturbed by adding estimates of the SST uncertainty. At this stage there is no implementation of ocean or coupled singular vectors to account for uncertainties in the ocean state. It is difficult to predict if the use of such singular vectors or stochastic physics in the ocean component of the model would result in a more accurate spread and more reliable seasonal forecasts than the current ECMWF system, however work in this direction is currently in progress. It is clear that whilst singular vectors for predictability study can still help our understanding of the climate system, their use in operational forecasts on long timescales has not yet been explored.

3.3. **The Thermohaline Circulation and Decadal Forecasting**

Griffies & Bryan (1997) showed that the internal variability of North Atlantic ocean temperature and meridional overturning circulation (MOC or often referred to as the thermohaline circulation) in a coupled ocean-atmosphere GCM is potentially predictable up to a couple of decades ahead. Subsequently, a vast number of studies devoted to the decadal predictability of ocean variability in the Atlantic sector have emerged (e.g., Sutton & Allen 1997, Boer 2000, Pohlmann et al. 2004, Sutton & Hodson 2005, Collins et al. 2006). Many of these studies are performed by constructing ensembles of coupled ocean-atmosphere numerical simulations in which each run corresponds to a randomly perturbed atmospheric state while leaving the ocean state unchanged. The spread of the individual model trajectories gives a measure of potential predictability. Since the ocean initial conditions are not perturbed, such results are considered an upper limit on the predictability. Not surprisingly, different studies show large discrepancies in the potential predictability of the Atlantic ocean variability. Moreover, while models indicate some degree of potential predictability of the ocean in the Atlantic sector, it is unclear how much of this predictability is imparted to the atmosphere.

Decadal prediction is a relatively new field compared to seasonal forecasting and numerical weather prediction (Goddard 2012) and many issues still need to be considered. In addition to the disparities between models, the verification of decadal forecasts is rather limited and our understanding of sources of error is poor. The development of initialised decadal prediction systems assimilating ocean observations has been the focus of many groups over the past several years and some improvement in this area has been made (Smith et al. 2007, Keenlyside et al. 2008). However, the studies often disagree on the magnitude and sign of regional changes, especially in the North Atlantic. The difference could involve model drift due to the initialisation shock (Doblas-Reyes et al. 2011), uncertainty in ocean observations and model error.

Given that the predictability arises from the dynamics of the large-scale ocean circulation, one therefore wonders how errors in ocean initial conditions or in ocean

model parametrisations can affect the predictability in the North Atlantic region. Our understanding of the processes governing the error growth of anomalies is still incomplete, yet recent results suggest that the ocean initial state remains important in the North Atlantic even on decadal times before the predictability arising from the boundary conditions (external forcing) becomes dominant (Branstator & Teng 2010, Branstator et al. 2012). In those studies, the predictability in the North Atlantic in various coupled GCMs is estimated using relative entropy from information theory. Yet, growth of anomalies calculated using singular vectors can provide valuable information regarding the predictability of the large-scale ocean circulation, upper ocean heat content before non-linearities and forcing become important. Over the past decade, singular vectors studies have been exploring the dynamics of error growth in the Atlantic and providing a potential framework for initialising decadal predictions.

Using 2D idealised models, early studies showed the value of studying singular vectors in relation to the predictability of the North Atlantic circulation and its predictability associated error growth in the initial state (Lohmann & Schneider 1999, Tziperman & Ioannou 2002, Zanna & Tziperman 2005, Alexander & Monahan 2009). Such studies showed that errors in ocean circulation can grow substantially on decadal timescales due to the non normality of the dynamical operator. Such simple models can describe the basics properties of the ocean circulation and are useful as proof of concept, allowing for an extensive analysis of the dynamics of error growth. However they can violate basic assumptions such as geostrophy. As mentioned earlier, the computation of singular vectors in complex coupled climate models solving the full primitive equation is extremely difficult. We will summarise two different approaches to calculate the ocean singular vectors of primitive equation models for decadal forecast.

Tziperman et al. (2008) and Hawkins & Sutton (2009) used the linear inverse modeling approach (Penland & Sardeshmukh 1995) to approximate the error growth associated with the MOC and explore its predictability in two different state-of-the-art CGCMs. A few steps are required to approximate the three-dimensional ocean singular vectors of such coupled climate models, given that the tangent linear and adjoint operators are not available. First, a reduced space based on empirical orthogonal functions (EOFs) of temperature and salinity anomaly fields in the Atlantic from the output of a control run is constructed. Second, under the assumption that the dynamics of this reduced space is linear, the propagator of the system is evaluated and the singular vectors of domain integrated energy and MOC are computed. Using the GFDL CM2.1 (Delworth et al. 2006), Tziperman et al. (2008) studied in details the growth of ocean temperature, salinity and MOC anomalies using singular vectors for lead times of 1 to 50 years. The singular vectors can grow significantly over a period of 5 to 10 yr, providing an estimate of the initial value predictability of the North Atlantic ocean circulation in this model. It is important to remember that severe truncation of the EOF-space can potentially lead to an underestimate of the error growth. The spatial structure of the leading singular vectors in this model indicates a large sensitivity to anomalies at high latitudes especially at the boundary between the subtropical and
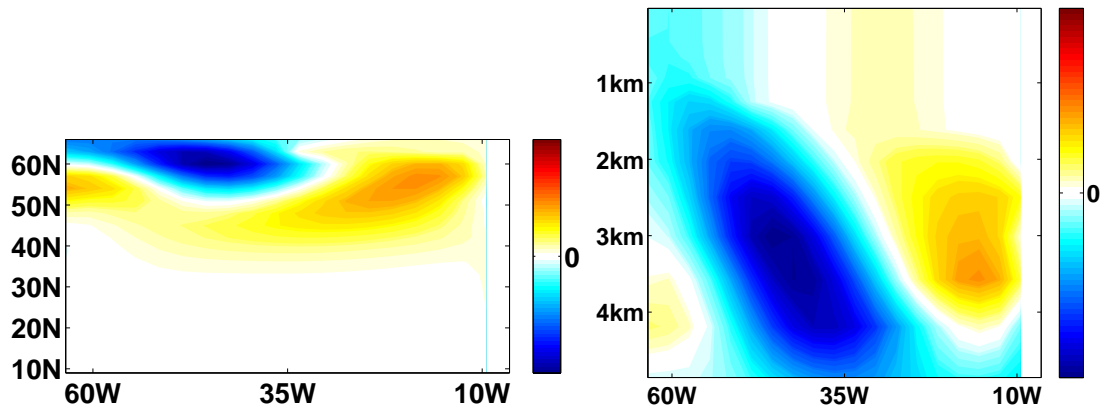
Figure 3. Spatial pattern of leading singular vector: (left) Longitude-depth cross section of density at 60N; (right) longitude-latitude cross section of density at 3km-depth. From Zanna et al. (2011).

subpolar gyres and in the subpolar gyre, therefore those regions should be properly initialised in any decadal prediction system. The study of Hawkins & Sutton (2009) using HadCM3 yields to similar results regarding the spatial patterns of the singular vectors however their results exhibit strong amplification in the Mediterranean sea and longer predictability times of temperature and energy. The methodology presented in Tziperman et al. (2008) and Hawkins & Sutton (2009) may be used to produce initial perturbations to the ocean state that may result in a stricter estimate of ocean predictability and ensemble spread than the common procedure of initialisation with perturbed atmospheric state and an identical ocean state (with or without assimilation of ocean observations). Recently, using HadCM3, the UK Met Office in an idealised perfect model set of predictability experiments showed that the spread and skill of the MOC increases when the ensemble is initialised with the singular vectors as opposed to simply perturbing the atmospheric states and accounting for ocean observational errors (Ed Hawkins, personal communication).

The analysis of the dynamics of error growth associated with the ocean state for decadal predictions remains extremely difficult in coupled GCMs. One can turn to GCMs in idealised configurations for such purposes. Zanna et al (2011, 2012) investigate the limits of predictability of the MOC and upper ocean temperatures due to errors in ocean initial conditions and model parametrisations in an idealised configuration of the ocean MIT general circulation model (MITgcm; Marshall et al. 1997). The singular vector spectrum for different initial and final norms is computed explicitly using traditional tools: adjoint and tangent linear models and Lanczos algorithms. The three-dimensional spatial structures of the leading singular vectors on decadal timescales is characterised by high-latitude deep density perturbations in the northern part of the basin (Fig. 3). The maximum growth rate of the perturbations occurring after 7.5 yrs is a result of a conversion of mean available potential energy into potential and kinetic
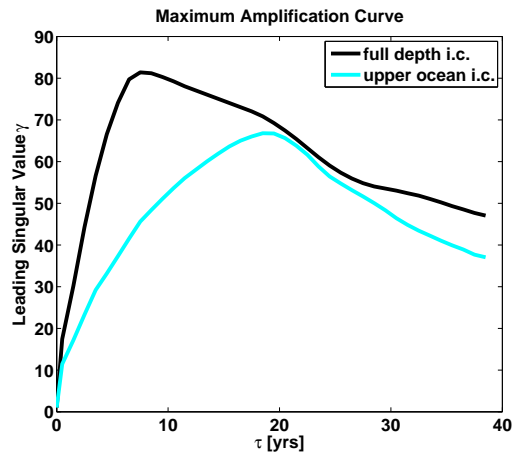
Figure 4. Maximum amplification curves: Leading singular value as function of lead time when maximising MOC error growth by constraining the singular vectors to the upper ocean (cyan curve) and when allowing the initial perturbations at all depths (black curve). From Zanna et al. (2012).

energy of the perturbations, reminiscent of baroclinic instability. The time scale of growth of MOC anomalies can be understood by examining the time evolution of deep zonal density gradients, which are related to the MOC via the thermal wind relation. The velocity of propagation of the density anomalies, found to depend on the horizontal component of the mean flow velocity and the mean density gradient, determines the growth time scale of the MOC anomalies and therefore provides an upper bound on the MOC predictability time due to the initial state. If the singular vectors are constrained to the upper ocean, the maximum growth is found at about 18.5 years (Fig. 4). This timescale of 18.5 years is longer than the 7.5 years obtained when the perturbations are allowed over the entire ocean depth. This result implies that the predictability timescales of 10 to 20 years obtained when only atmospheric perturbations are used to initialise ensemble experiments (e.g., Griffies & Bryan 1997, Pohlmann et al. 2004) may be overestimates as uncertainty in the ocean initial state is important. In addition to the difference in growth timescales, the MOC anomaly appears to be less sensitive to upper ocean perturbations than to deeper ones, at least in this model. While the ocean model is idealised in its configuration, it solves the primitive equations and one could use the singular vectors of this idealised GCM to initialise ensemble decadal predictions as done in numerical weather predictions.

While the model results can vary significantly, some results seem robust: basin integrated energy anomalies in the North Atlantic grow significantly in less than a decade, the singular vectors are concentrated at high latitudes, and the subpolar gyre, zonal advection and Rossby wave propagation are involved in the dynamics of error growth of temperature and salinity. The findings indicate that errors in ocean initial conditions or in model parametrisations or processes (deep convection, overflows etc...), particularly at high-latitudes and at depth, may significantly reduce the Atlantic ocean

circulation and climate predictability time to less than a decade. Yet, it remains unclear what the actual skill of MOC prediction is as very few observations are available. Recently, however, statistical methods to evaluate the actual forecast skill, as opposed to potential predictability, of North Atlantic SST using the observed record determined that forecast are skillful only for up to 5 years (Wunsch 2012, Zanna 2012). These statistical methods could be used as benchmarks to evaluate the skill generated from initialised ensemble decadal predictions in the current generation of climate models. It is clear that more work remains to be done by the decadal forecasting community at the theoretical and implementation levels to assess the sources of errors due to model parametrisations, initial state and initialisation shock. Singular vectors could be proven useful to explore those sources of errors.

4. Conclusions. SVs and the Future of Ensemble Forecasting

The predictability of weather and climate has been traditionally studied by investigating the error growth due to initial conditions, more specifically the growth rate of such errors and the associated state space patterns of maximum growth. The approach, pioneered by Lorenz, is concerned with the divergence of initially close dynamical trajectories measured by the Lyapunov exponents and vectors which can in some limits be described by the singular vectors of the dynamical system.

The maximum error growth associated with the singular vectors can reduce the large number of degrees of freedom of the high dimensional dynamical system which help the predictability analysis. Several studies showed that the normal mode instability was inadequate to analyse the dynamical instability of atmospheric flows (e.g., the PNA) due to the non-normality of the linearised dynamics and that singular vectors could provide a more accurate representation of forecast errors. Since the late 1980s, singular vectors have been implemented in the operational ensemble prediction system (EPS) on the assumption that they span the important directions of error growth. For the EPS, the singular vectors calculations are made from a numerical weather prediction model using tangent linear and adjoint models and an iterative Lanczos algorithm.

In addition to atmospheric variability, the analysis of singular vectors has proven extremely useful to study the predictability of other problems related to the dynamics of the ocean and atmosphere on timescales of seasons to decades. Two examples of such climatic phenomena are presented in the paper: the coupled ocean-atmosphere interannual variability in the tropical Pacific, El Niño and the Southern Oscillation (ENSO); and the large-scale decadal variability of the ocean meridional overturning circulation in the North Atlantic. For such problems the uncertainty in the initial state of the ocean remain important for the predictability of the events. In the case of ENSO, poor knowledge of surface and subsurface information in the Tropical Pacific can limit the seasonally dependent predictability the events. In the case of the Atlantic ocean circulation, the participation at high latitudes of the subpolar gyre and Rossby waves seems to determine the predictability of the decadal fluctuations of the circulation.

Further results implied that imperfect knowledge of the ocean initial state at high-latitudes at depth could be prove detrimental to decadal forecasts. Such regions are often linked to the dynamics of the large scale flow and the critical processes involved are parametrised.

While the singular vectors remain relevant (as long as the linearity assumption is valid) for the predictability of seasonal and decadal climate problems, there are several limitations associated with their computation in numerical models and their implementation at the operational level. The main problems discussed in the paper include: (1) the growth of perturbations on fast timescales which are irrelevant on climatic timescales and would dominate the solutions of singular vectors; (2) the computational cost of the singular vectors as the dimensions of the problem grow (large domains, additional prognostic variables) including the availability of adjoint and tangent linear models and (3) computation of an initial norm consistent with initial condition uncertainty, i.e. an analysis error covariance metric. Several approaches to tackle those issues and estimate the singular vectors for seasonal and decadal predictions are discussed however their use to account for initial uncertainties in the ocean component remains be fully explored and tested. Some work on these topics is in progress.

Our observing system is improving, data is being assimilated into atmospheric and ocean models, new parametrisations are been implemented including stochastic physics to represent model uncertainty. Moreover, the use of singular values is not obsolete in operational weather forecast. The implementation of stochastic parametrisations in the Ensemble Data Assimilation (EDA) shows that a considerable part of the initial uncertainty in medium rage forecast actually arises from model uncertainty in the data assimilation suite. The notion that model uncertainty contributes substantially to initial uncertainty is one of the justification for the use of singular vectors as a way to perturb initial conditions as part of an ensemble weather forecast. Using the EDA-based perturbations with the EPS enable a 50% reduction in the amplitude of the singular vectors operationally but it has not been possible to eliminate them completely. It is possible that they may not be needed in the future as the stochastic parametrisations improve and the development of correlated observation error statistics are made. However, even if singular vectors are dropped operationally in ensemble weather forecasts, they will continue to play a major diagnostic role for predictability and the development of ensemble prediction systems for weather and climate.

Alexander J & Monahan A H 2009 *J. Phys. Oceanogr.* **39**(2), 369–386.

Barkmeijer J, Van M G & Bouttier F 1998 *Q. J. R. Meteorol. Soc.* **124**, 1695–1713.

Beltrami E 1873 *Giornate di Matemetiche ad Uso degli Studenti Delle Universita* **11**, 98–106.

Bjerknes V 1904 *Meteorol. Z.* **21**, 1–7.

Blumenthal M B 1991 *J. Climate* **4**(8), 766–784.

Boer G J 2000 *Clim. Dyn.* **16**(6), 469–477.

Bonavita M 2011 *ECMWF 2011 Seminar Proceedings* .

Branstator G & Teng H 2010 *J. Climate* **23**(23), 6292–6311.

Branstator G, Teng H, Meehl G A, Kimoto M, Knight J R, Latif M & Rosati A 2012 *J. Climate* **25**(6), 1827–1846.

Buizza R, Miller M & Palmer T N 1999 *Q. J. R. Meteorol. Soc.* **125**(560), 2887–2908.

Buizza R & Palmer T N 1995 *J. Atmos. Sci.* **52**(9), 1434–1456.

Cane M A 1986 *Ann. Rev. Earth Planet Sci.* **14**, 43–70.

Chen D, Zebiak S E, Busalacchi A J & Cane M A 1995 *Science* **269**, 1699–1702.

Chen Y Q, Battisti D S, Palmer T N, Barsugli J & Sarachik E S 1997 *Mon. Weath. Rev.* **125**(5), 831–845.

Collins M, Botzet A, Carril A F, Drange H, Jouzeau A, Latif M, Masina S, Otteraa O H, Pohlmann H, Sorteberg A, Sutton R & Terray L 2006 *J. Climate* **19**(7), 1195–1203.

Delworth T L, Broccoli A J, Rosati A, Stouffer R J, Balaji V, Beesley J A, Cooke W F, Dixon K W, Dunne J, Dunne K A, Durachta J W, Findell K L, Ginoux P, Gnanadesikan A, Gordon C T, Griffies S M, Gudgel R, Harrison M J, Held I M, Hemler R S, Horowitz L W, Klein S A, Knutson T R, Kushner P J, Langenhorst A R, Lee H C, Lin S J, Lu J, Malyshev S L, Milly P C D, Ramaswamy V, Russell J, Schwarzkopf M D, Shevliakova E, Sirutis J J, Spelman M J, Stern W F, Winton M, Wittenberg A T, Wyman B, Zeng F & Zhang R 2006 *J. Climate* **19**(5), 643–674.

Doblas-Reyes F, Balmaseda M A, Weisheimer A & Palmer T N 2011 *J. Geophys. Res.* **116**, D19111.

Ehrendorfer M 1994*a* *Mon. Weath. Rev.* **122**, 703–713.

Ehrendorfer M 1994*b* *Mon. Weath. Rev.* **122**, 714–728.

Errico R M 1991 Theory and application of nonlinear normal mode initialization Technical Report NCAR/TN-344+IA National Center for Atmospheric Research Boulder, Colorado.

Farrell B 1988 *J. Atmos. Sci.* **45**, 163–172.

Farrell B 1989 *J. Atmos. Sci.* **46**, 1193–1206.

Farrell B 1990 *J. Atmos. Sci.* **47**(20), 2409–2416.

Farrell B F 1982 *J. Atmos. Sci.* **39**(8), 1663–1686.

Farrell B F 1985 *J. Atmos. Sci.* **42**, 2718–2727.

Farrell B F & Ioannou P J 1993*a* *Physics of Fluids a-fluid Dynamics* **5**(9), 2298–2300.

Farrell B F & Ioannou P J 1993*b* *J. Atmos. Sci.* **50**(14), 2201–2214.

Farrell B F & Ioannou P J 1995 *J. Atmos. Sci.* **52**(10), 1642–1656.

Farrell B F & Ioannou P J 1996 *J. Atmos. Sci.* **53**, 2025–2040.

Goddard L 2012 *Clim. Dyn.* **submitted**.

Griffies S M & Bryan K 1997 *Science* **275**(5297), 181–184.

Gu D & Philander S G H 1997 *Science* **275**(7), 805–807.

Hartmann D L, Buizza R & Palmer T N 1995 *J. Atmos. Sci.* **52**(22), 3885–3894.

Hawkins E & Sutton R 2009 *J. Climate* **22**(14), 3960–3978.

Jordan C 1874 *Memoire sur les formes bilineaires* **19**, 35–54.

Keenlyside N S, Latif M, Jungclaus J, Kornblueh L & Roeckner E 2008 *Nature* **453**(7191), 84–88.

Kleeman R, Tang Y M & Moore A M 2003 *J. Atmos. Sci.* **60**(23), 2856–2868.

Kug J S, Ham Y G, Kimoto M, Jin F F & Kang I S 2010 *Clim. Dyn.* **35**(2-3), 331–340.

Latif M, Anderson D, Barnett T, Cane M, Kleeman R, Leetmaa A, O'Brien J, Rosati A, & Schneider E 1998 *J. Geophys. Res.* **103**(C7), 14,375–14,393.

Latif M & Graham N E 1992 *J. Phys. Oceanogr.* **22**, 951–962.

Lau N C & Nath M J 2000 *J. Climate* **13**, 4287–4309.

Lawrence A R, Leutbecher M & Palmer T N 2009 *Q. J. R. Meteorol. Soc.* **135**, 1695–1713.

Lohmann G & Schneider J 1999 *Tellus A* **51**(2), 326–336.

Lorenz E N 1963 *J. Atmos. Sci.* **20**(2), 130–141.

Lorenz E N 1969 *Tellus* **21**, 289–307.

Marshall J, Adcroft A, Hill C, Perelman L & Heisey C 1997 *J. Geophys. Res.* **102, C3**, 5,753–5,766.

Molteni F, Buizza R, Palmer T N & T.Petroliagis 1996 *Q. J. R. Meteorol. Soc.* **122**, 73119.

Moore A M & Kleeman R 1996 *Q. J. R. Meteor. Soc.* **122**, 1405–1446.

Moore A M & Kleeman R 1997*a* *Q. J. R. Meteor. Soc.* **123**, 953–981.

Moore A M & Kleeman R 1997*b* *Q. J. R. Meteor. Soc.* **123**, 983–1006.

Moore A M & Kleeman R 1999 *Journal of Climate* **12**(10), 2965–2982.

Mureau R, Molteni F & Palmer T N 1993 *Q. J. R. Meteorol. Soc.* **119**, 299–323.

Murphy J M & Palmer T N 1986 *Meteorol. Mag.* **15**, 337–344.

Nastrom G D & Gage K S 1985 *J. Atmos. Sci.* **43**, 857–870.

Neelin J D, Battisti D S, Hirst A C, Jin F F, Wakata Y, Yamagata T & Zebiak S 1998 *Special Joint issue of J. Geophys. Res. Atmospheres and J. Geophys. Res. Oceans* **103**(C7), 14,261–14,290.

Palmer T N 1988 *Q. J. R. Meteorol. Soc.* **114**, 691–713.

Palmer T N 2000 *Reports On Progress in Physics* **63**(2), 71–116.

Palmer T N 2001 *Q. J. R. Meteorol. Soc.* **127**, 279–304.

Palmer T N 2012 *Q. J. R. Meteorol. Soc.* **138**, 841–861.

Palmer T N, Gelaro R, Barkmeijer J & Buizza R 1998 *J. Atmos. Sci.* **55**, 633–653.

Penland C & Sardeshmukh P D 1995 *J. Climate* **8**(8), 1999–2024.

Philander S G H 1986 *Nature* **322**, 236–238.

Pohlmann H, Botzet M, Latif M, Roesch A, Wild M & Tschuck P 2004 *J. Climate* **17**(22), 4463–4472.

Rosati A, Miyakoda K & Gudgel R 1997 *Mon. Weath. Rev.* **125**, 752–772.

Smith D M, Cusack S, Colman A W, Folland C K, Harris G R & Murphy J M 2007 *Science* **317**(5839), 796–799.

Suarez M J & Schopf P S 1988 *J. Atmos. Sci.* **45**, 3283–7.

Sutton R T & Allen M R 1997 *Nature* **388**(6642), 563–567.

Sutton R T & Hodson D L R 2005 *Science* **309**(5731), 115–118.

Talagrand. O & Courtier P 1987 *Q. J. R. Meteorol. Soc.* **113**, 1311–1328.

Tang Y, Kleeman R & Miller S 2006 *J. Climate* **19**(14), 3361–3377.

Thépaut J N & Courtier P 1991 *Q. J. R. Meteorol. Soc.* **117**, 1225–1254.

Thompson C J & Battisti D S 2000 *J. Climate* **13**, 2818–2883.

Thompson C J & Battisti D S 2001 *J. Climate* **14**(4), 445–466.

Trefethen L N, Trefethen A E, Reddy S C & Driscoll T A 1993 *Science* **261**(5121), 578–584.

Tziperman E & Ioannou P J 2002 *J. Phys. Oceanogr.* **32**(12), 3427–3435.

Tziperman E, Zanna L & Penland C 2008 *J. Phys. Oceanogr.* **38**(3), 588–604.

Wunsch C 2012 *Deep Sea Research* . In Press.

Xue Y, Cane M A, Zebiak S E & Blumenthal M B 1994 *Tellus* **46A**, 512–528.

Zanna L 2012 *J. Climate* **25**(15), 5047–5056.

Zanna L, Heimbach P, Moore A M & Tziperman E 2011 *J. Climate* **24**(2), 413–427.

Zanna L, Heimbach P, Moore A M & Tziperman E 2012 *Q. J. R. Meteorol. Soc.* **138**, 500–513.

Zanna L & Tziperman E 2005 *J. Phys. Oceanogr.* **35**(9), 1593–1605.